

Partitioning, Rotational Correlation, and Spin–Lattice Relaxation of Small Spin Probes in Dispersions of a Triglyceride Membrane

Kouichi Nakagawa

RI Research Center, Fukushima Medical University, 1 Hikarigaoka, Fukushima 960-1295

Received February 6, 2004; E-mail: nakagawa@fmu.ac.jp

The partitioning, rotational correlation times (τ_R), and electron spin–lattice relaxation times (T_{1e}) of various small spin probes in dispersions of a triglyceride membrane were investigated using CW-ESR (continuous wave-electron spin resonance) and SR (saturation recovery) spectroscopies. The partitioning of small spin probes, DTBN and TEMPO, in the aqueous and vesicle phases was determined by an ESR linewidth simulation. The results suggest that DTBN and TEMPO have a similar partitioning in the vesicle phase throughout the temperatures studied. The simulation results were quite different from those of conventional intensity analysis. In addition, the rotational correlation times of the vesicle phase for both probes varied from 1.2×10^{-10} to 4.9×10^{-10} s. The activation energy (E_a) calculated from the τ_R values in the phase was ~29 [kJ/mol] for the probes. The thermal behavior based on the E_a value is that in between the 12-doxylstearic acid (12-DSA) and 16-DSA moieties of the membrane. The longer τ_R and shorter T_{1e} (~0.33 μs) values of DTBN in the vesicle phase were obtained, and could be attributed to the probe environment in the membrane. Thus, the present experimental evidence has provided a qualitative understanding of the probe dynamics as well as the membrane properties.

The ESR (Electron Spin Resonance) spin probe methodology is advantageous for studying molecular dynamics in biological membranes on time scales from nanoseconds to milliseconds.[1,2] Changes in the probe motion are reflected in the ESR linewidth because of anisotropy in the *g*-value and in the nitrogen hyperfine structure. The lineshape of the ESR signal can be analyzed to determine the rotational correlation time (τ_R). The τ_R of a small spin probe in aqueous dispersions of lipid molecules is difficult to calculate. The spin probe exists at two sites: the aqueous and vesicle phases; conventional 9 GHz ESR can not differentiate between the two phases. Advanced ESR techniques, such as saturation recovery (SR), can be used to extract information about each phase separately. The electron spin–lattice relaxation time (T_{1e}) obtained by SR provides insight concerning the processes by which spin probes exchange energy with their surrounding membrane chains. That is, the T_{1e} values provide the overall tumbling mobility of the probe in the membrane. The combination of ESR and SR spectroscopic techniques could lead to descriptions of the membrane fluidity, dynamics, and translational diffusion.[3–7] However, limited studies of the advanced techniques used in biological membranes have been made.

Triglycerides are one of the three principal foodstuffs, together with carbohydrates and proteins. Poly(oxyethylene) hydrogenated castor oil (termed HCO), derived from one of the lipids and related natural products, has a unique chemical structure of triglyceride. It consists of a uniform fat structure embodying oxyethylene groups unlike most naturally occurring triglycerides, which are composed of three mixed fatty portions. Thus, HCO is an ideal amphiphilic membrane used to investigate membrane dynamics. Conventional and advanced ESR investigations of the membrane can provide a detailed understanding of the bilayer behavior as well as its dynamic structure. Moreover, the thermal behavior is one of the central roles of the bilayer to understand the membrane properties.

In a previous investigation, HCO was found to be a natural nonionic (amphiphilic) surfactant that forms vesicles.[8] A stable multi-lamellar vesicle with an average diameter of ~500 nm was observed. Furthermore, detailed motions including chain ordering of aliphatic spin probes in the membrane were investigated.[9–11] Chain ordering obtained by a slow-tumbling computational analysis for various spin probes in the membrane revealed that the probe moiety of 12-doxylstearic acid (12-DSA) (doxyl: 4,4-dimethyl-3-oxazolidinyloxyl) is relatively flexible. The terminal region of the membrane has very high fluidity, which is supported by a shorter T_{1e}. The T_{1e} values become shorter when the position of the probe moves toward the inner membrane. ESR and SR studies also provided dynamic information regarding the different types and rates of motion in the membrane.

In this investigation, the physicochemical properties, such as the partitioning, rotational correlation times (τ_R), and electron spin–lattice relaxation times (T_{1e}) of various small spin probes in aqueous solution containing a dispersion of HCO, were investigated. Overlapped and linewidth altering ESR signals of the aqueous and vesicle phases were analyzed using a linewidth-calculated program to determine the partitioning. The activation energy calculated using the τ_R values can be associated with the segmental micro-viscosity around the spin probes in the membrane. Further molecular dynamics of the spin probes was studied by SR. The correlation times of the probes are also discussed in relation to T_{1e}.

Materials and Methods

Materials. Poly(oxyethylene) (10) hydrogenated castor oil (termed HCO) of the highest grade was donated by Nikko Chem-

Published on the web July 9, 2004; DOI 10.1246/bcsj.77.1323

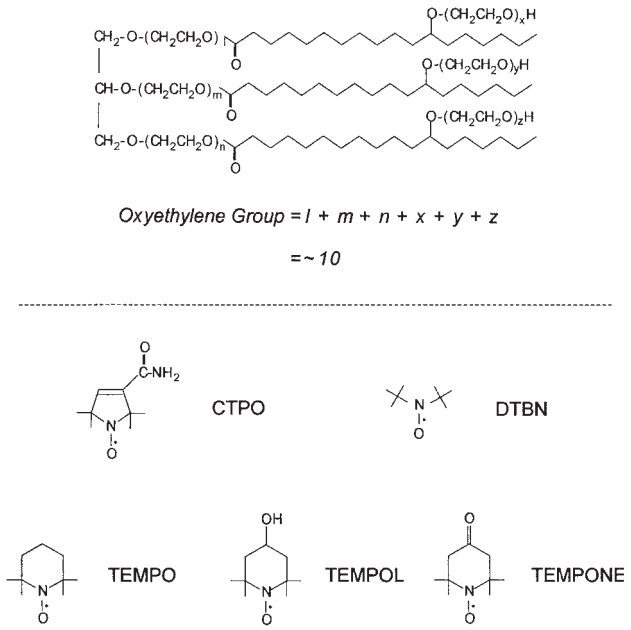

Fig. 1. Chemical structures of poly(oxyethylene) hydrogenated castor oil (HCO) and various nitroxide spin probes. The number of oxyethylene groups in the HCO used in this investigation was approximately 10.

icals Co. Ltd. (Tokyo, Japan) and used as received. The HCO had about 10 moles of oxyethylene moieties per mole of the compound. The spin probes, di-*t*-butyl nitroxide (DTBN), 2,2,6,6-tetramethylpiperidin-1-oxyl (TEMPO), 4-hydroxy-2,2,6,6-tetramethylpiperidin-1-oxyl (TEMPOL), 4-oxo-2,2,6,6-tetramethylpiperidin-1-oxyl (TEMPONE), and 3-(aminomethyl)-proxyl (CTPO) (proxyl: 2,2,5,5-tetramethyl-1-pyrolidinyloxyl), were obtained from Aldrich Chemical Co. and used as received. The chemical structures of the HCO and the spin probes used in this study are depicted in Fig. 1.

Sample Preparations. Two sample preparations were used at ambient temperature. Method one: A weighed amount of HCO was dissolved in a few milliliters of chloroform.[12] The weighed spin probe was dissolved in ~0.3 mL of chloroform and mixed with the HCO chloroform solution. After evaporation of the chloroform in a rotary evaporator, a 10 wt % dispersion of the HCO/spin probe in distilled water (HPLC grade, Nacalai tesque, Japan) was prepared. One aliquot of the dispersion solution was used for the ESR measurements. The final concentration of the spin probe was approximately 10 μmol dm^{-3} for the CW (continuous wave) ESR and 100 μmol dm^{-3} for the saturation recovery (SR) measurements. It is noted that slightly different doping concentrations of the small spin probes did not change the HCO properties.

Method two: HCO was dispersed in water to ~10 wt %, and a spin probe was added to the solution. A test tube containing the dispersion solution was agitated on a vortex mixer until completely dispersed. The final concentration of the spin probe was the same as that in method one. For CW ESR measurements, the dispersion solution was placed in a glass capillary (i.d. 0.9 mm) and one end was sealed.

Deoxygenation. For CW ESR, the sample solution (~0.15 mL) was deoxygenated for about 15 min in an AtmosBag (Aldrich, U.S.A.), and the solution was put into a capillary (i.d., 0.9 mm; o.d., 1.4 mm; Nippon Rikagaku Kikai Co. Ltd., Japan). The sample capillary was inserted into a 3-mm ESR tube (JEOL Datum) in the AtmosBag.

Degassing of the previous SR measurements was carried out using a gas-permeable plastic capillary, known as TPX.[6,7,13] For this investigation, Teflon tubes to achieve degassing were used in the following manner. Two Teflon tubes were inserted side-by-side in a 4-mm ESR tube. One Teflon tube (i.d., 0.96 mm; o.d., 1.56 mm) contained the sample solution. Nitrogen was passed through the second Teflon tube (i.d., 1.5 mm; o.d., 2 mm) to purge oxygen from the solution. Detailed descriptions are given elsewhere.[9]

CW ESR Measurements. ESR measurements were made with a 9 GHz JEOL FE 1XG spectrometer with a TE_{011} cylindrical cavity. The sample temperature was controlled by nitrogen gas flow through the Dewar vessel using a JEOL ES-DVT system. The ESR signals were digitized using a Scientific Software Services data-acquisition system (Illinois, U.S.A.). The microwave frequency was measured using an EMC-14 X-band microwave frequency counter (Echo Electronics Co., Ltd., Japan). Typical conditions were as follows: microwave frequency, 9.185 GHz; microwave power, 10 mW; modulation amplitude, 0.08 mT; time constant, 0.1 s; sweep rate, 0.312 mT per minute.

CW ESR Linewidth Simulation. The overlapped ESR signal from different environments was simulated by the linewidth calculation. The linewidth can vary under certain probe environments. When line broadening arises from incomplete averaging of the *g*-factor and the hyperfine coupling interactions in the limit of rapid tumbling in solution, the linewidth varies with the magnetic quantum number (M) from one component to the next across the spectrum. The dependence of the linewidth of an individual hyperfine line is given in the motional narrowing region by the following expression:[14,15]

$$\Gamma = A + BM_I + CM_I^2, \tag{1}$$

where Γ is the linewidth, M_I is the nuclear spin quantum number, and A, B, and C are the functions of nitrogen *g*-factor and hyperfine tensor. It is noted that the A term contributes to the overall spectrum, the B term causes an anisotropy in the spectrum, and the C term broadens the spectrum symmetrically. In the simulation, parameters (A, B, and C) were changed to obtain the best-fit simulated spectra. The best-fit spectra were chosen based on minimization of the residual between the experimental and simulated spectra. Based on the simulated spectra of the two phases, aqueous and vesicle, the partitioning of spin probes at each temperature was determined.

Rotational Correlation Time. Various methods have been developed for determining the correlation time for the molecular motion based on changes in the amplitude, position, and widths of the ESR lines.[14,15] A small molecule in an aqueous dispersion generally has a rotational correlation time (τ_R) on the order of $\sim 10^{-10}$ s. The time scale of τ_R can be estimated from the spectra of a nitroxide spin probe using the following expression:[16–19]

$$\tau_R = \left(\frac{2\sqrt{3}g_{iso}\beta_e}{\hbar b^2}\right)\left(\sqrt{\frac{I_0}{I_{+1}}} + \sqrt{\frac{I_0}{I_{-1}}} - 2\right)\Delta H_{pp0}, \tag{2}$$

where β_e is the electron Bohr magneton, $\hbar$ is Plank's constant, I is amplitude of a peak, and subscripts +1, 0, and −1 are the nuclear quantum numbers for ^{14}N. ΔH_{pp0} is the peak-to-peak linewidth of the centerline. The values of g_{iso} and b are calculated from the parameters for immobilized spin probe:

$$g_{iso} = \frac{1}{3}(g_{xx} + g_{yy} + g_{zz}), \tag{3}$$

$$b = \frac{2}{3}\left[A_{zz} - \frac{1}{2}(A_{xx} + A_{yy})\right]. \quad (4)$$

Calculations of τ_R for the spin probes were made using the magnetic principal values.[20] The parameters I_{+1}, I_0, I_{-1}, and ΔH_{pp0} obtained from the experimental spectra were used to calculate τ_R. It is noted that Eq. 2 is used for the relatively fast motion of small spin probes, but not for the slower motion of various aliphatic spin probes.

Saturation Recovery Measurements. The electron spin–lattice relaxation time (T_{1e}) was measured by a home-built saturation recovery (SR) spectrometer at the University of Denver.[21] A 5-loop-4-gap resonator (LGR) was used.[22] The sample temperature was monitored with a thermocouple positioned immediately above the resonator. The magnetic field for recording the recovery signal was set on the high-field nitrogen hyperfine line for the probe in the vesicle or aqueous phase. Artifacts were removed by subtracting an instrumental background response that was measured with the magnetic field set 10 mT higher than for the signal. The data were collected with a pump time of 5 μs, which was long relative to the recovery time constants and relative to the tumbling correlation times. Under these conditions, the contribution to the recovery due to spectral diffusion is minimized and the time constant is assigned as T_{1e}. The detailed experimental settings are also given elsewhere.[9,19]

Results and Discussion

CW ESR of Spin Probes. The CW ESR spectrum of the spin probe (DTBN) in aqueous dispersions consists of two overlapping signals, as presented in Fig. 2(A). The contributions from the two triplets are best resolved for the high-field hyperfine line. The ESR lines from the probe in the vesicle phase are broader than those from the aqueous phase. The molecular motions of the spin probe in the vesicle are somewhat restricted. In addition, the ESR spectrum obtained from

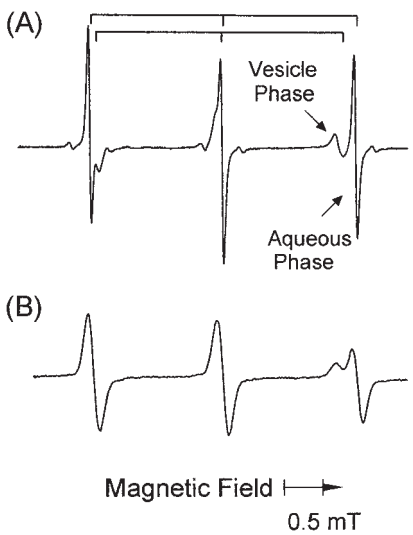

Fig. 2. The ESR spectra of (A) DTBN and (B) TEMPO in aqueous dispersions of HCO. Schematic description regarding the ESR spectra comprising the two triplets: a part of the probe is in the vesicle phase and the remaining is in the aqueous phase. The two sets of hyperfine lines, which are resolved for the high-field hyperfine line, are marked in (A).

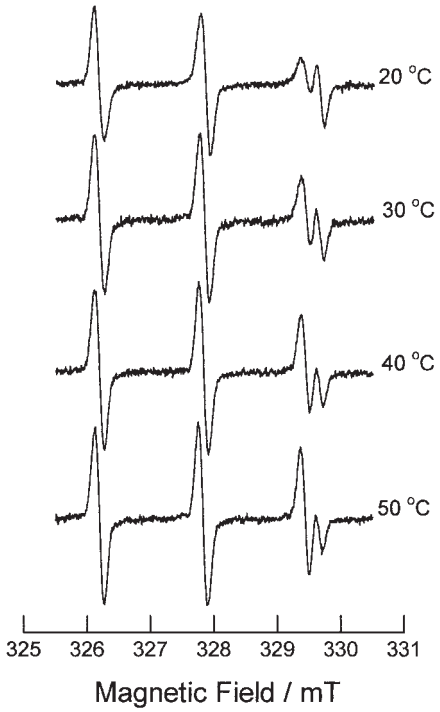

Fig. 3. Temperature dependence of the ESR spectra for the spin probe (TEMPO) in aqueous dispersions of HCO. The temperatures at which the spectra were obtained are indicated.

DTBN/HCO/H_2O shows relatively sharp ESR lines. The spectral difference between the aqueous and vesicle phases is more noticeable than that for TEMPO (Fig. 2).

Figure 3 shows the ESR spectra of the TEMPO/HCO/H_2O system. ESR signals of spin probes between the aqueous and vesicle phases were measured as a function of the temperature. Focusing on the high-field lines, the signal amplitude of the vesicle phase increases as the temperature increases. The vesicle intensity becomes dominant above ~40 °C. Similar ESR observations were obtained for the DTBN/HCO/H_2O system.

The ESR spectra of the probe partitioning between the two phases were analyzed using the simulation program (Eq. 1), which takes into account the linewidth change. The percent of the partitioning was determined by calculating the aqueous and vesicle signals. The representative best-fit spectra along with the experimental spectra are presented in Fig. 4. The obtained partitioning of the spin probes is plotted as a function of the temperature in Fig. 5. The error mainly comes from the sample preparations at ambient temperature as well as a slight difference between the observed and calculated spectra. The simulation results suggest that the partitioning of DTBN and TEMPO in the vesicle phase is similar. The partitioning (~50%) of the probe at 15 °C increases to 74% at the higher temperature, and shows no abrupt change (Fig. 5). Moreover, the partitioning for both probes shows a similar temperature behavior, and can be in direct relation to the membrane properties. These results are quite different from the previously reported values, which were calculated using the peak intensities.[8b] There are two main reasons for the discrepancy. First, the true vesicle intensity is not the same for the overlapped resultant signal. Second, the linewidths of the probe in the vesicle vary

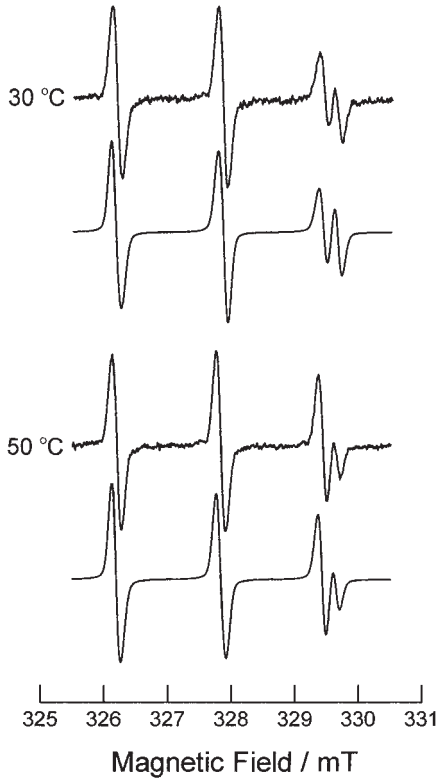

Fig. 4. The representative experimental and simulated ESR spectra for TEMPO in aqueous dispersions of HCO.

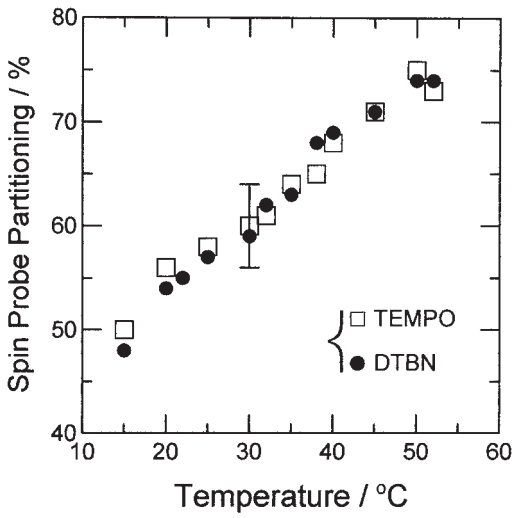

Fig. 5. Partitioning of the vesicle phase for DTBN (●) and TEMPO (□) in H_2O dispersions of HCO as a function of the temperature.

when the tumbling motion changes.

When TEMPONE and TEMPOL in the dispersions were examined in a similar manner to those for DTBN and TEMPO, no distinguishable vesicle peak for both at different temperatures was found. Only the nitrogen triplet was observed. The ESR hyperfine splitting suggests that both TEMPONE and TEMPOL might remain in the aqueous phase, or might have very small g-value and hyperfine differences in the two phases.

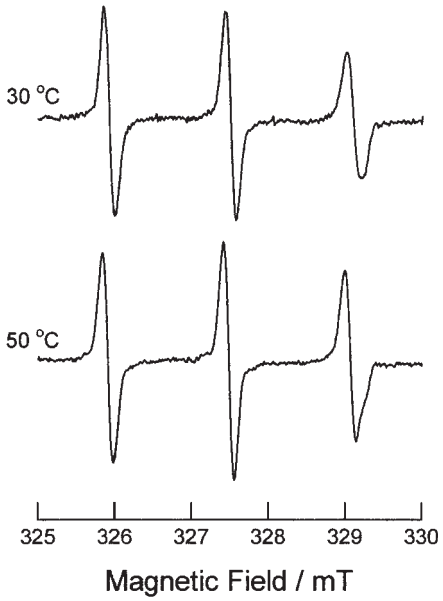

Fig. 6. The representative ESR spectra of the vesicle phase. The ESR spectra were obtained by the subtraction of TEMPO aqueous peaks.

In order to analyze the tumbling motion of the spin probes in the vesicle phase, the rotational correlation time (τ_R) was calculated using Eq. 2. The molecular tumbling time in the slightly slow fluctuation regime ($\sim 10^{-10}$ s) can be estimated by the expression. The equation can be used to evaluate the motional behavior of spin probes in the membrane. The ESR spectra of the vesicle phase were obtained by subtracting two spectra under the same experimental temperature and ESR conditions. The reference spectra were used by dissolving spin probes in H_2O. The subtraction was able to eliminate the aqueous peaks. Also, the subtraction was examined with slightly different doping concentrations of the probe. It is noteworthy that slightly different doping concentrations of the probe do not affect the HCO properties. However, it is true that one must have a good reference spectrum for the subtraction method. The representative ESR spectra obtained after subtraction are shown in Fig. 6. Based on the subtracted ESR spectrum, the τ_R was calculated. The value of τ_R for DTBN changes from 1.2×10^{-10} to 4.9×10^{-10} s at the temperatures studied. The value of τ_R for TEMPO changes from 1.2×10^{-10} to 4.2×10^{-10} s. The longer correlation time ($\sim 4.2 \times 10^{-10}$ s) is an indication of ESR line broadening, especially for the high-field line. This also proves that one should not use peak intensity analysis.

The temperature dependence of the rotational correlation times for DTBN and TEMPO in the vesicle phase is presented as a function of the inverse of the absolute temperature in Fig. 7. It is notable that the correlation time and the partitioning show no drastic change throughout the temperatures studied. An Arrhenius-type equation gives the activation energy for the spin probe in the phase,

$$\tau_R = {\tau_R}^0 \exp\left(\frac{E_a}{RT}\right), \tag{5}$$

where E_a is the activation energy, R is the gas constant, and T is the absolute temperature. The slopes of the plots give the acti-

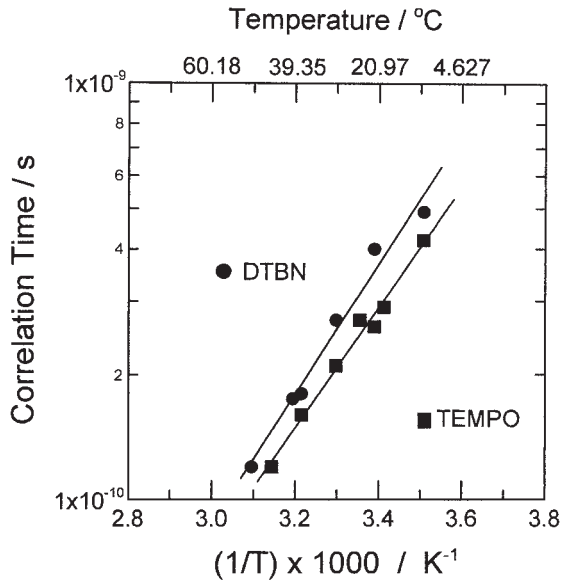

Fig. 7. Temperature dependence of the rotational correlation times for the spin probes, DTBN (●) and TEMPO (■), in the vesicle phase is plotted as a function of the inverse absolute temperature. The activation energies were calculated from the slopes.

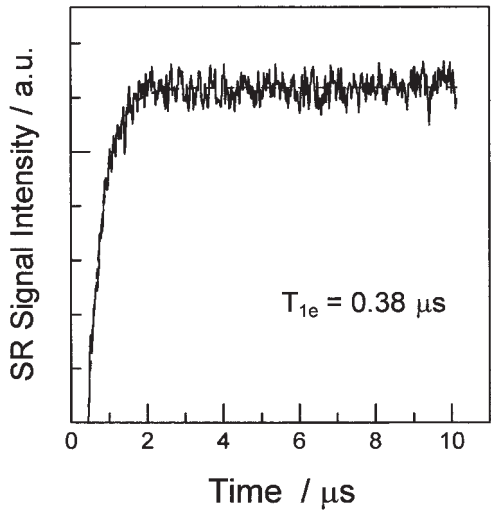

Fig. 8. The typical saturation recovery signal of DTBN in the vesicle phase at 22 °C. The applied magnetic field was set on the magnetic field that corresponds to the maximum intensity in the first-integral spectrum for the vesicle comportment. The dotted line indicates a single-exponential fit to obtain T_{1e}.

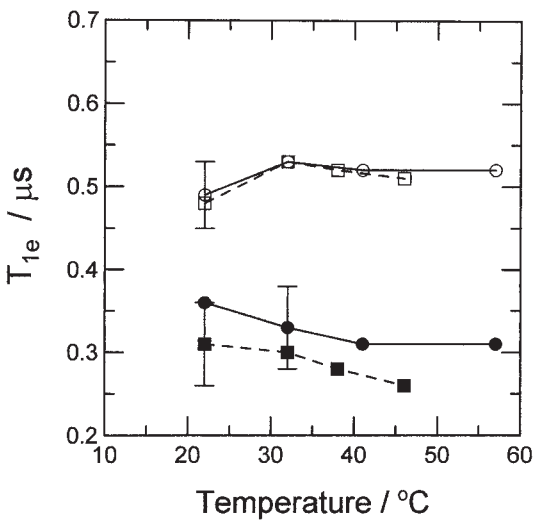

Fig. 9. Plot of T_{1e} for DTBN in H_2O (circles) and D_2O (squares) dispersions as a function of the temperature. The open circle and open square represent T_{1e}'s in the aqueous phase. The filled circle and filled square represent T_{1e}'s in the vesicle phase.

vation energies (Fig. 7). The activation energies obtained for TEMPO and DTBN in the membrane are 27.6 ± 1.7 and 29.7 ± 1.7 [kJ/mol], respectively. The results suggest that both thermal motions are similar in the membrane. Moreover, the E_a of ~29 [kJ/mol] is that in between 24 [kJ/mol] of 12-DSA and 37 [kJ/mol] of 16-DSA of the membrane.[9] The activation energy implies that the probe moiety has a similar temperature behavior as well as an approximate location in the membrane.

The calculated τ_R for TEMPONE of the TEMPONE/HCO/H_2O system is approximately 5×10^{-11} s, and is independent of the temperature in the range of 20–50 °C. The value of τ_R is close to the free rotational tumbling time. The estimated τ_R from the spectra for TEMPO and DTBN in the aqueous phase was close to the value. Similar results were obtained for TEMPOL at the same temperature range. The correlation times of TEMPOL and TEMPONE in the dispersions were one order of magnitude faster than that for TEMPO in the vesicle phase.

Spin–Lattice Relaxation Time (T_{1e}) of Small Spin Probes. In order to further examine the probe motion in the vesicle phase, a direct observation of the interaction between the spin probe and the lattice (membrane) was attempted using SR. The interaction of the probe contributes to the relaxation time in the membrane. T_{1e}'s for the probes in the aqueous and vesicle phases were measured at a magnetic field corresponding to the maximum intensity in the first-integral spectrum for each of the components of the high-field hyperfine line. The typical SR signal from the vesicle peak in the DTBN/HCO/H_2O system at 22 °C is presented in Fig. 8. A single-exponential fit to the experimental data is shown by the dotted line. At this temperature, the signal-to-noise ratio of the SR signal from the vesicle phase is poorer than that for the aqueous phase because of a weaker ESR intensity.

The T_{1e}'s of the probes in the vesicle phase showed a very weak temperature dependence in the examined range (Fig. 9). The τ_R value of $\sim 10^{-10}$ s (Fig. 7) predicts that T_{1e} is in the vicinity of the minimum value. The minimum value occurs when $\tau_c \omega_0 \approx 1$, where τ_c is the correlation time and ω_0 is the 9 GHz ESR resonance frequency.[23] The temperature dependence of T_{1e} is normally low around this regime. The values of T_{1e} in the vesicle phase are about 0.33 μs in the dispersions. The values of T_{1e} in the aqueous phase are around 0.52 μs. The relaxation time for DTBN in the aqueous phase is consistent with a shorter τ_R in the phase. The T_{1e} values for TEMPO in the aqueous and vesicle phases are about 0.47 μs.[19] There is no clear T_{1e}

difference between the two phases, because the overlap of two signals is more significant than that for DTBN (Fig. 2).

The T_{1e} of DTBN in the vesicle phase is shorter than that for the aqueous phase, even considering the experimental error. The shorter T_{1e} ($\sim$0.33 μs) in the vesicle phase can be due to an interaction between the probe and the host lattice. No drastic change in T_{1e} as a function of the temperature was observed. This implies a continuous change of the probe moiety with increasing temperature. The results are attributable to the thermal property of the membrane. In addition, the shorter T_{1e} for DTBN in the vesicle phase could be interpreted as resulting from the location of the probe in the hydrophobic portion of the membrane. This would be consistent with the location of DTBN in the hydrophobic portion of the lipids, as determined by NMR.[24] Thus, a relatively longer τ_R and a shorter T_{1e} for DTBN in the vesicle phase are attributed to the membrane environment. The comparative inhibition of the tumbling motion might account for the obtained results. It is noteworthy that the relaxation also depends not only on the tumbling mobility of the probe, but also on the local concentration. The difficulty is both the local mobility and the concentration change as a function of the temperature.

In order to verify the hydration and/or dehydration effect, T_{1e} of spin probes in a D_2O dispersion solution was measured. Figure 9 also shows a plot of T_{1e} for DTBN in D_2O dispersions. The T_{1e} values of DTBN for the two phases are similar to the case of H_2O. The present SR measurements on T_{1e} of the probes did not show any clear evidence of it based on the results regarding the dispersions of HCO in H_2O and D_2O. Moreover, the recent investigation of aliphatic spin probes in H_2O and D_2O dispersions show no clear difference.[9] Thus, the result suggests that the relaxation process with interaction of H_2O or D_2O is not the major contribution.

The T_{1e} values of TEMPO in the aqueous and vesicle phases are 0.42–0.51 μs throughout the temperatures studied. The values of T_{1e} for both phases are very close. As discussed earlier in this section, the two signals from aqueous and vesicle phases at the high-field line significantly overlap (Fig. 2). Even though the applied magnetic field was set on each different peak, the recovery signal may not be reliable for each phase. However, based on the correlation times, the relaxation time of TEMPO in the vesicle phase could show a longer value than that for DTBN.

Finally, the simultaneous observation of the two different signals along with the linewidth change at various temperatures is a perplexing problem for conventional ESR. In order to obtain further information about membrane dynamics, analyses of the overlap signals from the two different environments (the aqueous and vesicle phases) were attempted using 9 GHz ESR and SR spectroscopies. Despite the problems, new physicochemical evidence was extracted by the combination of various approaches. It would be more advantageous to utilize the higher resonance frequency to gain a better separation of spectra with slightly different g-values.[25]

Conclusions

The ESR and SR spectroscopic methods provide detailed information regarding the partitioning, rotational correlation, and relaxation time of the spin probes in a triglyceride membrane. The partitioning of DTBN and TEMPO in the vesicle phase, using a linewidth simulation, is about 50% at 15 °C, and increases with an increase in the temperature. The partitioning for both probes showed a similar temperature dependence. The results were quite different from the conventional peak intensity analysis. In addition, the rotational correlation times of the vesicle phase for the probes changed from 1.2×10^{-10} to 4.9×10^{-10} s. The longer tumbling time demonstrates that the ESR intensity analysis is not valid. The activation energy obtained by the correlation time was $\sim$29 [kJ/mol]. The E_a value implies that the thermal behavior of the probe is in between the 12- and 16-DSA moieties. The activation energy suggests the approximate probe location in the membrane. The longer τ_R and the shorter T_{1e} ($\sim$0.33 μs) of DTBN in the vesicle phase were obtained, and can also be attributed to the probe environment in the membrane. The obtained T_{1e} values suggest that the interaction between the probe and H_2O (or D_2O) does not contribute to the major relaxation process in the membrane. Therefore, the present ESR evidence using small spin probes has provided a further understanding of the membrane properties.

Part of this research was performed at the University of Denver. The author thanks Prof. Sandra S. Eaton for her generous gift of the simulation program and helpful discussion concerning the results.

References

1 "Spin Labeling, Theory and Applications," ed by L. J. Berliner, Academic Press, New York (1976).

2 G. R. Eaton and S. S. Eaton, "Biological Magnetic Resonance," ed by G. R. Eaton, S. S. Eaton, and L. J. Berliner, Plenum Press, New York (2000), Vol. 19, Chap. 2.

3 B. R. Patyal, R. H. Crepeau, and J. H. Freed, *Biophys. J.*, **73**, 2201 (1997).

4 Y. Lou, M. Ge, and J. H. Freed, *J. Phys. Chem. B*, **105**, 11053 (2001).

5 T. J. T. Pinheiro, P. J. Bratt, I. H. Davis, D. C. Doetschman, and A. Watts, *J. Chem. Soc., Perkin Trans. 2*, **1993**, 2113.

6 W. K. Subczynski, J. S. Hyde, and A. Kusumi, *Biochemistry*, **30**, 8578 (1991).

7 A. Kusumi, W. K. Subczynski, and J. S. Hyde, *Proc. Natl. Acad. Sci. U.S.A.*, **70**, 1854 (1982).

8 a) M. Tanaka, H. Fukuda, and T. Horiuchi, *J. Am. Oil Chem. Soc.*, **67**, 55 (1990). b) T. Horiuchi and K. Tajima, *J. Jpn. Oil Chem. Soc.*, **41**, 1197 (1992).

9 K. Nakagawa, *Langmuir*, **19**, 5078 (2003).

10 K. Nakagawa, *Chem. Lett.*, **2002**, 666.

11 K. Nakagawa, *Bull. Chem. Soc. Jpn.*, **77**, 269 (2004).

12 "Liposomes, A Practical Approach," ed by R. R. C. New, Oxford University Press, Oxford (1990), Chap. 2.

13 C.-S. Lai, L. E. Hopwood, J. S. Hyde, and S. Lukiewicz, *Proc. Natl. Acad. Sci. U.S.A.*, **79**, 1166 (1982).

14 D. J. Kivelson, *Chem. Phys.*, **33**, 1094 (1960).

15 R. Wilson and D. J. Kivelson, *Chem. Phys.*, **44**, 4440 (1966).

16 N. D. Chasteen and M. W. Hanna, *J. Phys. Chem.*, **76**, 3951 (1972).

17 A. L. Buchachenko, A. L. Kovarskii, and A. M. Vasserman, "Advances in Polymer Science," ed by Z. A. Rogovin, John Wiley & Sons, Inc., New York (1974), p. 26.

18 D. J. Schneider and J. H. Freed, "Biological. Magnetic Resonance," ed by L. J. Berliner and J. Reuben, Plenum Press, New York (1989), Vol. 8, Chap. 1.

19 K. Nakagawa, "EPR in the 21st Century: Basic and Applications to Material, Life and Earth Sciences," ed by A. Kawamori, J. Yamauchi, and H. Ohta, Elsevier, Amsterdam (2002), p. 494.

20 "Spin Labeling, Theory and Applications," ed by L. J. Berliner, Academic Press, New York (1976), Appendix II, p. 565.

21 R. W. Quine, S. S. Eaton, and G. R. Eaton, *Rev. Sci. Instrum.*, **63**, 4251 (1992).

22 G. A. Rinard, R. W. Quine, S. S. Eaton, G. R. Eaton, and W. Froncisz, *J. Magn. Reson., Ser. A*, **108**, 71 (1994).

23 "Principles of Magnetic Resonance," 3rd ed, P. C. Slichter, Springer-Verlag, Berlin (1990), Chap. 5.

24 J. A. Dix, D. Kivelson, and J. M. Diamond, *J. Membr. Biol.*, **40**, 315 (1978).

25 P. P. Borbat, A. J. Costa-Filho, K. A. Earle, and J. H. Freed, *Science*, **291**, 266 (2001).